

# **OPEN ACCESS**

# Effect of High Current Density Pulses on Performance Enhancement of Optoelectronic Devices

To cite this article: Md Hafijur Rahman et al 2024 ECS J. Solid State Sci. Technol. 13 025003

View the article online for updates and enhancements.

# You may also like

- Fluctuating hydrodynamics of dilute electrolyte solutions: systematic perturbation calculation of effective transport coefficients governing largescale dynamics Ryuichi Okamoto
- Understanding the mechanisms of electroplasticity from a crystal plasticity perspective Arka Lahiri, Pratheek Shanthraj and Franz Roters
- Effects of electrical pulse on metal deformation behaviors Tao Huang, Fan Yang, Bing-Hui Xing et al.



# Your Lab in a Box!

The PAT-Tester-i-16: All you need for Battery Material Testing.

- ✓ All-in-One Solution with integrated Temperature Chamber!
- ✓ Cableless Connection for Battery Test Cells!
- ✓ Fully featured Multichannel Potentiostat / Galvanostat / EIS!

www.el-cell.com +49 40 79012-734 sales@el-cell.com









# **Effect of High Current Density Pulses on Performance Enhancement of Optoelectronic Devices**

Md Hafijur Rahman, <sup>1</sup> Nicholas Glavin, <sup>2</sup> Aman Haque, <sup>1,z</sup> Fan Ren, <sup>3</sup> and Stephen J. Pearton <sup>4</sup>

Thermal annealing is commonly used in fabrication processing and/or performance enhancement of electronic and opto-electronic devices. In this study, we investigate an alternative approach, where high current density pulses are used instead of high temperature. The basic premise is that the electron wind force, resulting from the momentum loss of high-energy electrons at defect sites, is capable of mobilizing internal defects. The proposed technique is demonstrated on commercially available optoelectronic devices with two different initial conditions. The first study involved a thermally degraded edge-emitting laser diode. About 90% of the resulting increase in forward current was mitigated by the proposed annealing technique where very low duty cycle was used to suppress any temperature rise. The second study was more challenging, where a pristine vertical-cavity surface-emitting laser (VCSEL) was subjected to similar processing to see if the technique can enhance performance. Encouragingly, this treatment yielded a notable improvement of over 20% in the forward current. These findings underscore the potential of electropulsing as an efficient in-operando technique for damage recovery and performance enhancement in optoelectronic devices.

© 2024 The Author(s). Published on behalf of The Electrochemical Society by IOP Publishing Limited. This is an open access

© 2024 The Author(s). Published on behalf of The Electrochemical Society by IOP Publishing Limited. This is an open access article distributed under the terms of the Creative Commons Attribution 4.0 License (CC BY, http://creativecommons.org/licenses/by/4.0/), which permits unrestricted reuse of the work in any medium, provided the original work is properly cited. [DOI: 10.1149/2162-8777/ad28c8]

Manuscript submitted July 28, 2023; revised manuscript received January 10, 2024. Published February 21, 2024.

Supplementary material for this article is available online

Laser diodes are the core components of optical storage systems, photoacoustic spectroscopy, barcode readers and in optic communication systems. <sup>1-6</sup> Amongst distinct types of laser diodes, Verticalcavity surface-emitting laser (VCSEL) and edge-emitting laser diodes are most prominent. The main difference between these two diodes is the direction of emitted light. In the case of VCSEL device, the light emits perpendicular to the wafer surface, whereas the latter emits light parallel to the surface of the wafer. In addition, VCSELs have a much smaller wavelength drift with temperature compared to edge-emitting lasers (EEL) and the power consumption of a VCSEL is less compared to the EEL. <sup>1-3</sup>

Performance of optoelectronic devices depends on the quality of materials and manufacturing, among other variables. The defects in used materials, such as dislocations, vacancies, or impurities, introduce localized states and hinder carrier mobility and recombination rate, leading to reduced performance of electronic devices.<sup>7</sup> The defects in oxide layer of used semiconductor material is a major source of leakage current and degrades the microelectronic devices.<sup>8</sup> In addition, residual stresses might arise during the fabrication process due to a mismatch in thermal expansion coefficients between the various materials. 9,10 These stresses can deform the device structure and change the lattice parameters and bandgap, eventually impacting the electrical properties. <sup>11,12</sup> High contact resistance at the metal-semiconductor interfaces can impede efficient carrier mobility, resulting in power dissipation and an overall decrease in device performance. 13,14 Moreover, the inhomogeneous distribution of dopants during the doping of semiconductors can lead to non-uniform carrier density and mobility and affect the device's characteristics. 15 Among other variables, the suboptimal performance of electronic devices might come due to small geometric variations, <sup>16</sup> surface contamination, <sup>17</sup> and fabrication complexity. 18 In addition to fabrication errors, the exposure of electronic devices to harsh operating environments, such as elevated temperatures, bias conditions beyond the maximum rating, and other operational stresses, can lead to a progressive decrease in device

functionality. During the processing of most semiconductor photonic devices, convection oven type thermal annealing is usually performed to lower contact resistance, activate implanted dopants or reduce interfacial trap densities.<sup>19</sup> Other alternative treatments are rapid thermal annealing or microwave annealing which also can be used for the same purposes as described above.<sup>20</sup> All of these are performed during the processing of semiconductor devices to ensure high quality interfaces and sufficient material quality for device operation. Once the device is ready for intended use, high temperature exposure can lead to severe damage and/or significantly reduce performance.<sup>21,22</sup>

In this present work, a non-thermal annealing technique was applied that uses mechanical stimulus instead of elevated temperature. To do this, very high current density pulses are passed through the device at duty cycles of 0.008% or lower. The ultra-low duty cycle implies that the resulting thermal spikes are given enough time to dissipate in the solid without raising the temperature. The current pulses have two distinct types of scattering interactions with the lattice and defect. The lattice scattering causes Joule heating, which is effectively suppressed with our low duty cycle processing. The defect scattering gives rise to the electron wind force (EWF), which is mechanical in nature because it is derived from the loss of electron momentum when impinged to a defect. In the electro-migration literature, <sup>23</sup> the EWF is typically ignored in favor of thermal effects, however our approach harnesses the EWF to eliminate the thermal effects. This not only makes the EWF the dominant factor, but also amplifies its magnitude because significantly higher current density can be applied to the device without causing any thermal damage. We suggest that this makes the EWF potent enough to mobilize the defects at room temperature. Our proposed technique is ultra-fast compared to conventional thermal annealing, requiring less than a minute of processing time. Other than the pulsed power source, it requires only electrical interconnects, making it possible to process a device in-operando. This is a highly desired feature because thermal annealing requires a laboratory (or processing environment) and cannot be performed without placing the device in an oven. Similar processing has shown to enhance the mechanical and electrical properties of metallic materials, alloys and microelectronic devices. 24-26 It is well established that electropulsing

<sup>&</sup>lt;sup>1</sup>Department of Mechanical Engineering, The Pennsylvania State University, University Park, Pennsylvania 16803, United States of America

<sup>&</sup>lt;sup>2</sup>Air Force Research Laboratory, Wright-Patterson AFB, Ohio 45433, United States of America

<sup>&</sup>lt;sup>3</sup>Department of Chemical Engineering, University of Florida, Gainesville, Florida 32611, United States of America <sup>4</sup>Department of Materials Science and Engineering, University of Florida, Gainesville, Florida 32611, United States of

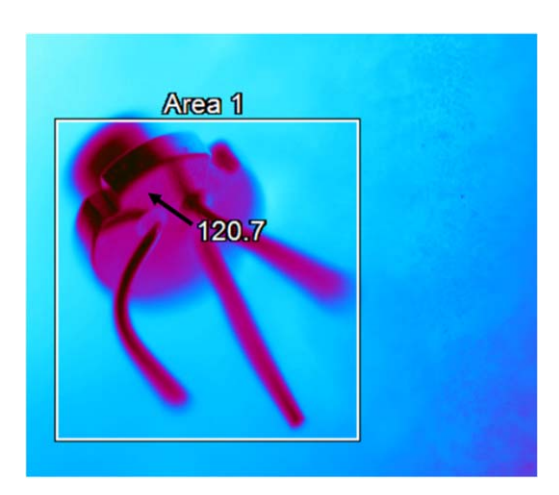


**Figure 1.** Thermograph showing the diode being stored at 120 °C (arrow indicating diode surface reaches around 120 °C) for 48 h.

can improve the microstructure or reduce bulk or interfacial defects. 27,28 It is important to note that the term electropulsing does not necessarily mean room temperature processing. Even a moderate duty cycle or inability to maintain a sharply defined pulse-width may increase temperature. The thermal domain is self-compounding; meaning it can increase defect concentration, which itself raises the temperature via increased electrical resistance; leading to a thermal runway. Therefore, it is important to note that our approach specifically aims to maintain ambient processing temperature, which has produced very encouraging results in the past. 29–31 Our proposed electro-pulsed annealing technique offers reduced thermal budget, minimizing the risk of material damage and preserving structural integrity, while ensuring rapid processing through short pulses of electrical current. The motivation for this study is that if successful, such an approach could also be useful for extending the useful lifetime of laser diodes by annealing defects created during operation.

## **Experimental**

This study is designed to examine the effectiveness of room temperature electropulsing as a degradation mitigating process. This is conducted in two parts, the first involving a commercially available edge emitting green laser diode (model PLT5 520B), which is intentionally degraded by storing it at an elevated temperature for a prolonged period of time. We then applied the room temperature electropulsing treatment to the device and characterized again to investigate the enhancement in performance (if any). The second part of the study involves a more challenging condition, where the techniques described herein were used to improve the performance of a fresh device. This part of the study was performed on a commercially available VCSEL (model EGA2000-850-N). In this case, it is assumed that defects or stress were introduced during fabrication and/or packaging and that our proposed processing removes some component of this defect population.

A commercial laser diode (PLT5 520B) was degraded intentionally by storing it at a higher temperature than its maximum storage temperature rating which is 80 degrees Celsius for this specific diode. The degradation process is carried out in several stages over a period of one week. The I-V characteristic curve was measured at each stage of the degradation process using a Keithley 2400 SMU and Kickstart software. First, the laser diode was stored at an ambient temperature of 120 °C for 48 h, then at ambient room temperature for 24 h. The same procedure was repeated for higher temperatures, i.e., 130 °C and 150 °C. An Optris PI-640 thermal microscope was used to measure the specimen temperature during the high temperature storage condition and is shown in Fig. 1. Given the long storage time, the laser diode inside the package is assumed

to come to the equilibrium temperature of the furnace. The initial I-V characteristic curve of the laser diode displayed a current of 300 mA for a voltage of 7 V, indicating its pristine condition (see, for example, Fig. 2). However, subjecting the diode to a high temperature of 120 °C for 48 h caused an 18.33% increase in forward current, with a subsequent I-V curve indicating a current of 355 mA for a voltage of 7 V. The increment in forward current due to its degradation is a result of defect introduction and increased nonradiative current which is described in later section. Then we stored the same diode at room temperature (20 °C) for 24 h and did the I-V characterization again. This revealed that the damage induced by storing the diode at 120 °C did not reverse to its pristine condition. Additional storage at 130 °C for 24 h resulted in a 33.33% degradation in forward current, with an I-V curve indicating a current of 400 mA for 7 V. To check the damage stability, we stored the diode at room temperature for another 24 h, and the I-V curve gave almost the same current (I = 399 mA) for 7 V, indicating that the damage was permanent. To further degrade the diode, it was stored at 150 °C for another 24 h, and the I-V curve showed I = 442 mA for 7 V, which was a 47.33% degradation as compared to the initial condition. Lastly, the stability for this step was also checked by storing the diode at room temperature for 24 h, and the I-V curve after this room temperature storage showed  $I = 440 \,\mathrm{mA}$  for 7 V, indicating that the damage was naturally irreversible.

#### Results and Discussion

Non-radiative recombination occurs when an electron and hole recombine without emitting a photon, which can cause a loss of carrier density in the active region of the diode since the process is trap-mediated.  $^{32,33}$  This loss of carrier density can increase the effective resistance of the diode, which can result in a higher forward current being required to maintain the same voltage across the device. According to Recombination Enhanced Defect Generation (REDG) model, non-radiative recombination events can generate defects within the semiconductor material, which can act as additional recombination centers and lead to further non-radiative recombination and hence further defect generation.  $^{34,35}$  According to this REDG model,  $I(t) = I_0 + I_{nr}(t)$ , where  $I_{nr}(t) = \beta e^{kt}$ , where,  $\beta$  is a material-dependent constant representing the initial non-radiative current  $I_{nr}(0)$ .

The degradation parameter k is described in Ref. 34 as  $k = e^{\left(\mu_0 - \frac{E_A}{K_b T}\right)}$ . is a scale parameter;  $E_A$  is the activation energy for defect generation, T is the temperature in the active zone and  $k_B$  is the Boltzmann constant. The active region temperature is an explicit function of thermal resistance  $(R_{th})$  and keeps a proportional relationship as  $T = T_{sub} + R_{th}(V.I - P)$ , where  $T_{sub}$ is the submount temperature, V and I are voltage and current across the laser diode, and P is the optical power. The high storage temperature causes thermal damage in a laser diode which in turn increases the thermal resistance  $R_{th}$  and so as the active zone temperature T. The degradation parameter k is large for a higher active zone temperature and thus the nonradiative current is also increased. Due to this high non-radiative current, the operating forward current is large for a thermally damaged laser diode. Figure 2c shows a semilogarithmic I-V curve, highlighting the threshold region. Due to thermal damage, a small (from 2.4 V to 2.55 V) shift in the threshold voltage is observed.

Electropulsing is found to be an effective method for rejuvenating thermally damaged laser diodes through electron defect interactions. To achieve this, the frequency of pulsed current was maintained at a constant 2 Hz, while the pulse width was varied between  $10~\mu\text{s}-40~\mu\text{s}$ . These parameters are chosen to suppress any rise in specimen temperature. The sharp pulse followed by a large pause (low frequency) before the next pulse helps us suppress the thermal spike. The controlled electropulsing treatment was found to be effective in reducing degradation levels caused by extended storage in a high temperature ambient environment, as measured by the change in forward current at a fixed voltage (7 V) from the as-

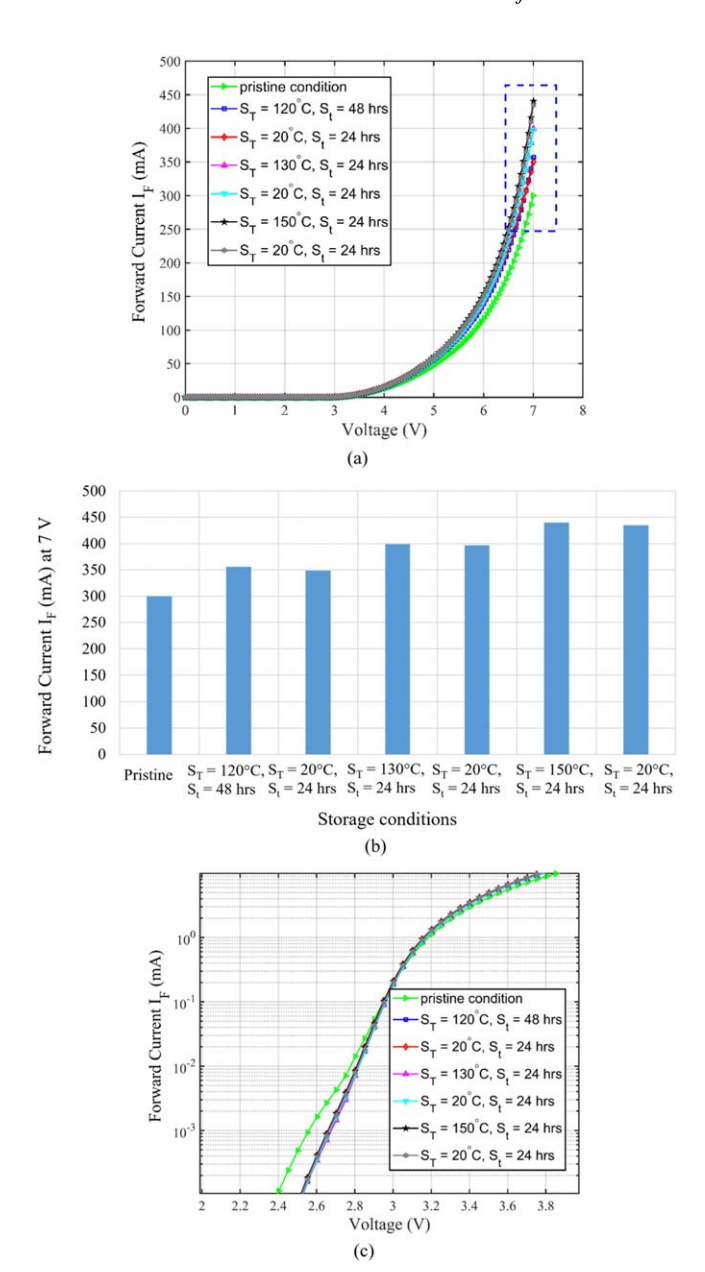


**Figure 2.** (a) I-V characteristic curves for the various stages of the degradation process due to long term, elevated temperature storage  $(S_T, S_t)$  represents the Storage Temperature and Storage time respectively), (b) Forward current for the various storage conditions at 7 V represented by bar graphs. (c) Semilog I-V curve in the threshold region.

received control value from (434.3 mA) 47.33% to as low as (323.2 mA) 7.7%. The electropulsing was carried out for 180 s for each set of parameters, and the I-V characteristic curves for the

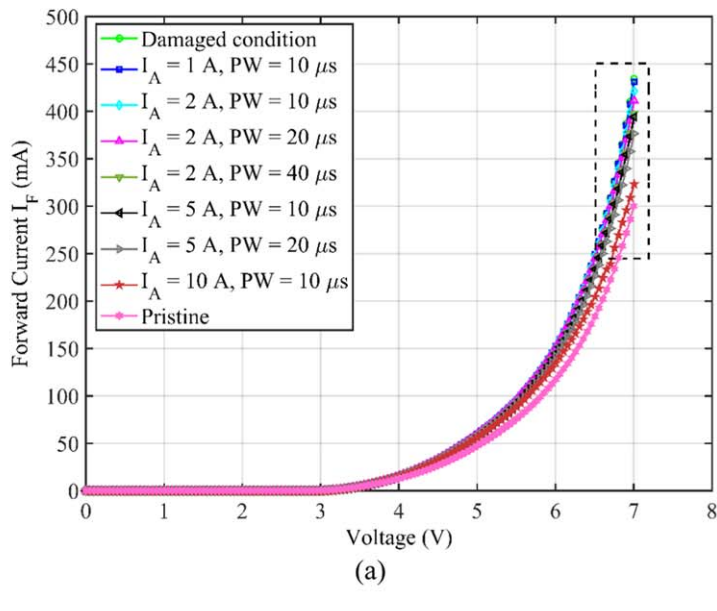
different electropulsing parameters are depicted in Fig. 3a, and the forward currents of the device at a specific voltage of 7 V for the various annealing parameters are shown in Fig. 3b. It is to be noted that the proposed annealing technique is similar to mechanical shock loading, analogous to blowing a leaf with wind. The electron wind force from the sharp pulses transfer the shock wave energy to the defects. Since defect motion is irreversible and depend on the input energy level, our technique needs only a few cycles (or seconds) of pulsing. Prolonged application of pulsing does not improve unless the energy (such as current density) is increased. Our earlier investigations consistently demonstrated marked improvements in device performance within a short pulsing duration. Specifically, in Ref. 31, we achieved rejuvenation of Ti/4H-SiC Schottky barrier diodes in just 30 s of pulsing. Likewise, when applying current pulsing to diverse materials and alloys, significant enhancements were observed with pulse durations of less than one minute<sup>29</sup> and 2 min.<sup>36</sup> These findings underscore the effectiveness of shorter pulsing durations in instigating favorable changes in device characteristics. The 180 s pulsing scheme is used in this study just to make sure that a steady-state has been reached.

It is observed that, up to a certain limit, the forward current decreases with increasing electropulsing current density. In the case of lower annealed current (IA) up to 2 A, the increased pulse width was found to improve the defect rejuvenation process. However, it is important to note that the maximum pulse width utilized was 40  $\mu$ s for lower annealed current ( $I_A = 2 A$ ), as higher pulse widths could rise up annealing temperature and generate joule heating.<sup>29</sup> For high annealed current ( $I_A = 5 A$  and above), the pulse width becomes more critical, as higher pulse width could lead to more joule heating. The minimum forward current was achieved at 10 A annealed current, and with a 10  $\mu$ s pulse width application. The increased forward current after thermal damage, ~47% (434.3 mA), was reduced to  $\sim$ 8% (323.2 mA) by optimized electropulsing treatment. The changes in forward current and associated recoveries in each step are shown in Table I. Note that the electropulsing does not fully restore the initial forward current condition prior to thermal degradation, but does reduce some of the excess current, indicating there is annealing of some of the thermally-induced defect population. Regarding the threshold voltage, we consistently observed that the electropulsing doesn't induce any shift from the damaged condition, and the threshold voltage remains constant across all cases (see Fig. 3c).

The next level of challenge was to examine whether the proposed electropulsing process would be effective on pristine devices. In this case, we do not expect significant enhancement in performance especially for optimized fabrication processing, device geometry and materials selection. For the pristine VCSEL device, increasing the forward current will increase the peak wavelength at which the laser emits most of its power.<sup>37</sup> The output power of a VCSEL is proportional to the current density in the active region. This is because the current density determines the number of carriers that are injected into the active region. The number of carriers in turn determines the gain of the device, which is proportional to the output power.<sup>38</sup> Therefore, increasing the forward current will increase the

Table I. The progress in damage recovered with various pulsing conditions.

Pulsing conditions Percentage damage remain in the sample (%)		Damage recovered (%)	
Pristine	_		
Damaged	44.76	_	
$I_{.} = 1 \text{ A}, PW = 10 \ \mu \text{s}$	43.70	2.38	
$I_{.}^{A} = 2 \text{ A}, \text{ PW} = 10 \ \mu\text{s}$	40.45	9.62	
$I_{.}^{A} = 2 \text{ A}, \text{ PW} = 20 \ \mu\text{s}$	37.12	17.07	
$I_{.}^{A} = 2 \text{ A}, \text{ PW} = 40 \ \mu \text{s}$	32.57	27.23	
$I_{.}^{A} = 5 \text{ A}, \text{ PW} = 10 \ \mu\text{s}$	31.38	29.89	
$I_{.}^{A} = 5 \text{ A}, \text{ PW} = 20 \ \mu\text{s}$	25.54	42.95	
$I_{.}^{A} = 10 \text{ A}, PW = 10 \mu \text{s}$	7.74	82.72	



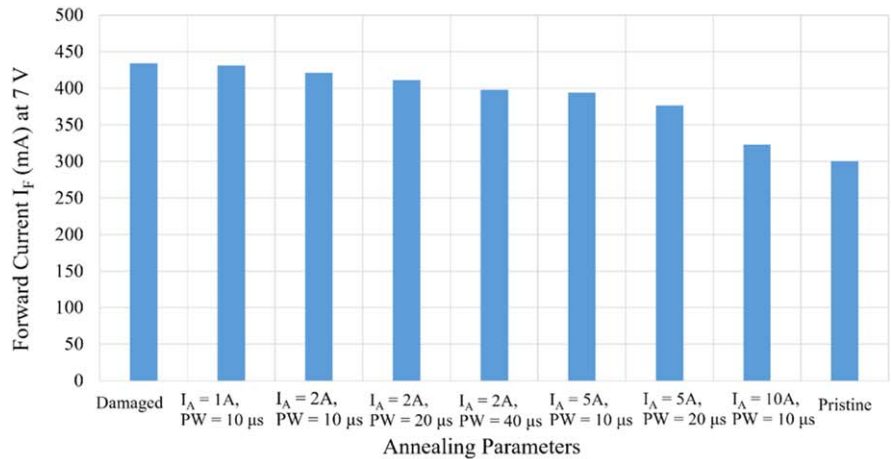
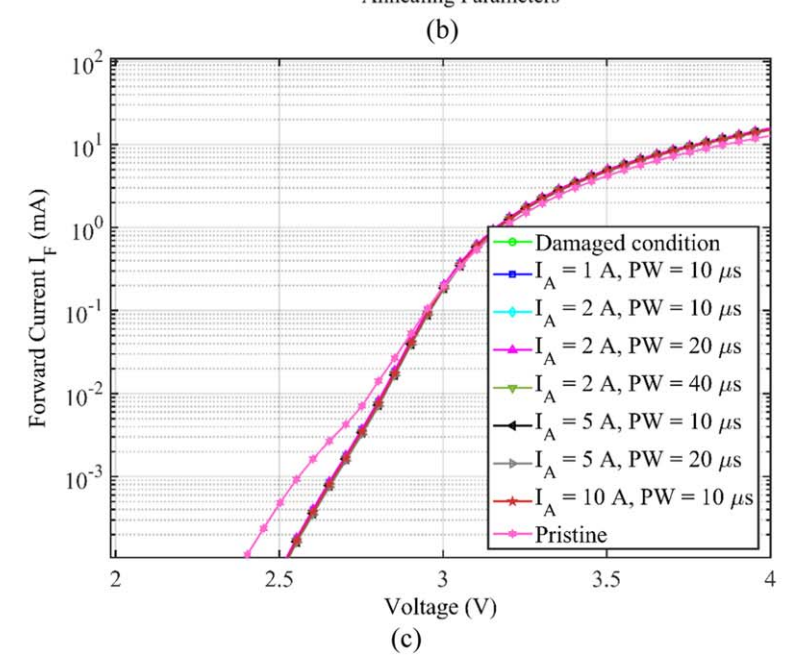


**Figure 3.** (a) I-V characteristic curves for various electropulsing conditions. PW denotes pulse width (b): Forward current at 7 V for various pulsing conditions presented by bar graphs. (c) Semilog I-V curve in the threshold region.



output power of a VCSEL. To investigate the effects of electropulsing, a series of experiments were conducted with a constant frequency of 2 Hz while varying the annealed current and pulse width. The results revealed significant changes in the forward

current, highlighting the impact of electropulsing on the device's behavior.

Figure 4a illustrates the I-V characteristic curves as a function of electropulsing conditions. For a closer examination of the forward

current changes with electropulsing conditions, a bar graph is shown in Fig. 4b which illustrates the output currents of VCSEL device at a forward voltage of 2.2 V under different annealing parameters. Initially, the VCSEL device operated with a forward current of 328 mA at 2.2 V. Upon subjecting the VCSEL to electropulsing, an initial reduction of 20.3% in the forward current was observed. We believe that such early-stage inconsistency in the process could originate from the metallic electrical terminals/contacts. It is documented in the literature that high rate of pulsing can refine the grains in metals, <sup>39,40</sup> particularly in metals with initial residual stress. In the absence of heating, the grains do not grow in size—but the internal dislocations decrease in density to form new grain boundaries, a process to recrystallize into smaller grains. It is therefore possible that the temporary increase terminal resistance influences the I-V characteristics of the entire device. For higher pulse widths, this effect diminishes since the metallic contact microstructure becomes less susceptible to the electrical pulses. From the device perspective, this decrease could be attributed to the population of existing traps in the active region of the laser, which affected the injection efficiency, carrier recombination rates, or carrier density within the active region, leading to the observed decrease in forward current.4

The observed change in forward current for various pulsing conditions have been shown in Table II.

As the annealed current was increased during subsequent experiments, a notable trend emerged. The forward current exhibited a gradual recovery and began to rise, surpassing its pristine (328.03 mA) condition by 24.94% (409.85 mA). This recovery can be attributed to the beneficial effects of electropulsing on this device, which annealed some of the trap states in the active and cladding regions. By increasing the annealed current, the device's performance improved as the electropulsing process facilitated the restoration of carrier injection efficiency, enhanced carrier recombination rates, and optimized carrier density within the active region. As a result, the forward current increased, leading to higher output power. Moreover, we have employed a semilogarithmic curve (see Fig. 4c), providing insights into the device's behavior at the threshold region, and observed that the threshold voltage exhibited no discernible changes subjecting to electropulsing.

The generalized finding of this study is that very short bursts of high current pulses generate mechanical force or shock in semiconductor devices that can mobilize and eliminate defects and traps. We do not envision this process to substitute the thermal annealing performed during device fabrication, but it can be an effective way to rejuvenate devices degraded over time or due to harsh operating conditions. This is because the proposed process can be performed in-operando, without the device being removed from deployed condition to be placed in a furnace, laser or microwave heating environment. Rather, only electrical terminals are needed, which are already present in semiconductor devices. The process is also very fast and takes place around room temperature. Another findings of this study is that higher current density with lower duty cycle provides the maximum improvement in device performance. This is because higher current density relates to higher electron wind force, which gives higher probability for defect mobilization and/or annihilation. However, there are some discrepancies observed in this trend. For example, in Fig. 3b, we observed I = 5 A, PW = 10  $\mu$ s performed slightly worse than I = 2 A, PW = 5  $\mu$ s. This discrepancy could be attributed to the impact of localized distribution of defect variations. We note that each of the pulsing conditions leaves a permanent effect on the specimen. It is plausible that, during the initial pulsing at I = 2 A, PW = 10  $\mu$ s, a localized defect or set of defects may have been triggered, temporarily impacting the device performance. Subsequently, in the next step (I = 5 A,  $PW = 10 \mu s$ ), the performance may exhibit a relative reduction due to the influence of these triggered defects. However, as the current intensity is increased in the subsequent stage (I = 10 A), the higher electron wind force generated may effectively annihilate these localized defects, again leading to a significant improvement in device

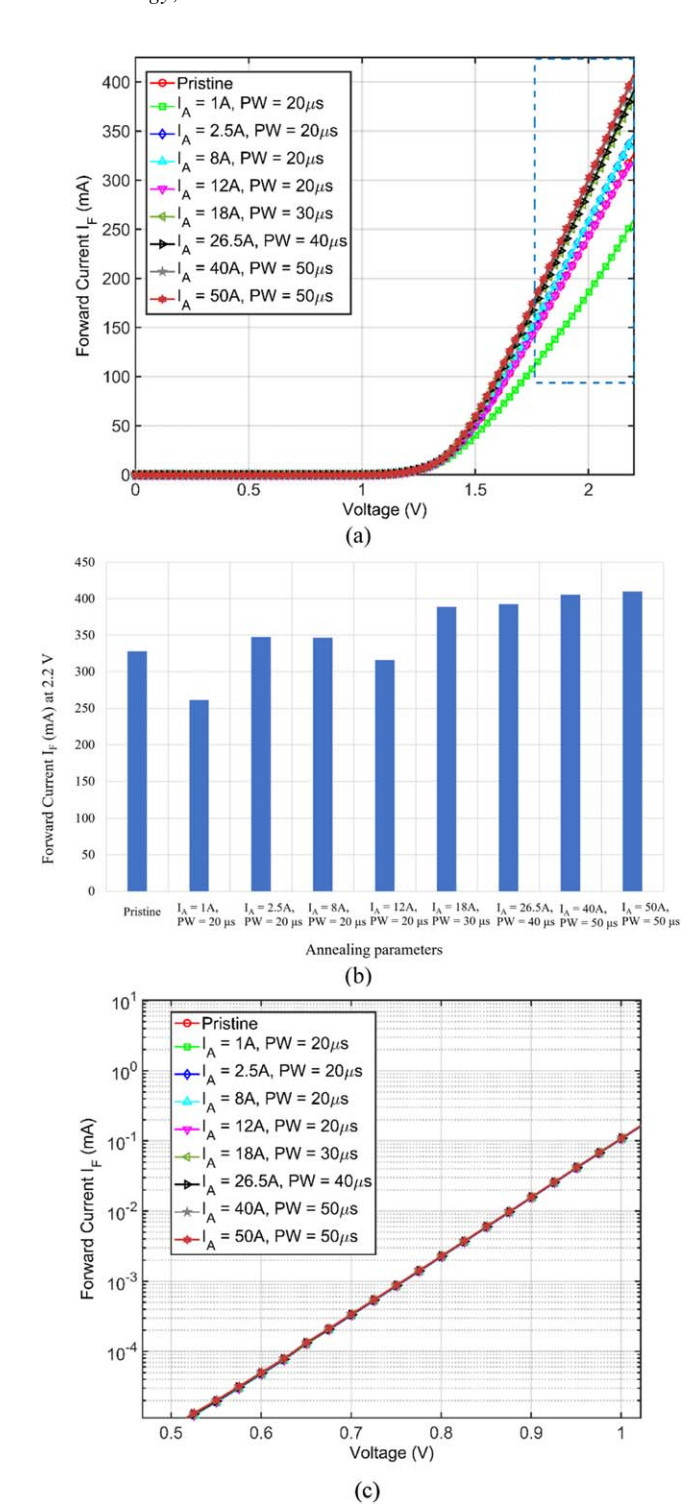


**Figure 4.** (a): I-V characteristic of VCSEL with various electro-pulsed annealing conditions. (b): Forward current at 2.2 V for various pulsing conditions presented by bar graphs. (c) Semilog I-V curve in the threshold region.

performance. Lower duty cycle implies negligible rise in temperature. We therefore kept the frequency to the lowest possible (2 Hz) with our experimental setup. At this frequency, current density effects are more dominant that pulse width, hence we kept pulse width fairly constant (10–40  $\mu\,\mathrm{s}$ ).

Earlier, we invoked an analogy of the electron wind force mobilizing defects to actual wind moving leaves (or light objects). It can be argued that the magnitude of the electron wind force

Table II. Percentage increment in forward current for various pulsing parameters.

Pulsing conditions	Percentage increase in performance (%
Pristine	_
$I_{A} = 1 \text{ A}, PW = 20 \ \mu \text{s}$	-20.32
$I_{A} = 2.5 \text{ A}, \text{ PW} = 20 \ \mu\text{s}$	5.97
$I_{\Delta} = 8 \text{ A}, \text{ PW} = 20 \ \mu\text{s}$	5.70
$I_{\Delta} = 12 \text{ A}, \text{ PW} = 20 \ \mu\text{s}$	-3.68
$I_{\Delta} = 18 \text{ A}, \text{ PW} = 30 \ \mu\text{s}$	18.53
$I_{A} = 26.5 \text{ A}, \text{ PW} = 40 \ \mu\text{s}$	19.71
$I_A = 40 \text{ A}, \text{ PW} = 50 \ \mu\text{s}$	23.63
$I_{A} = 50 \text{ A}, \text{ PW} = 50 \ \mu\text{s}$	24.94

dominates the defect annihilation effects, therefore one could start with the highest possible current density. This would, in principle, work—but only after a thorough study of the highest but safe current density. To demonstrate this, we performed another experiment where fresh VCSEL devices (from the same batch as presented in Fig. 4) were electropulsed, except this time the input current and pulse width applied were 50 A and 50  $\mu$ s in the very first step. The results, given in the supplementary information, are similar to the observations made in Fig. 4 where the currrent value was increased to to value in smaller increments. No matter how small the duty cycle is, there is always a risk of thermal runaway mode of failure risk associated with very large current density. In addition, the safe limit of highest current density would depend on device type, packaging conditions and ambient. Since thermal runaway is a highly non-linear risk phenomenon, for each types of devices, it is recommended that the study begins with a minimum current and systematically increased it to observe the corresponding improvements. Finally, the proposed process is not a monotonic function of these parameters. For example, too high current density can still damage a fresh device because of an uncontrollable thermal spike. Also, the initial condition is important albeit in a different way. If the device is too badly degraded (such as 50% reduction of current), the electropulsing technique may not be able to improve the condition substantially.

## Conclusions

Electropulsing has been successfully applied to rejuvenate a thermally damaged edge-emitting laser diode by leveraging electron defect interactions. A controlled electropulsing treatment with a frequency of 2 Hz and varying pulse widths (10–40  $\mu$ s) effectively reduced degradation in forward current from 47.33% to as low as 7.7%. The study demonstrated that the increased forward current due to thermal damage of an edge emitting laser diodes can be restored with increasing the electropulsing current density. In the second part of this study, we observed that the electropulsing of a pristine VCSEL device initially caused a reduction in forward current, likely due to trap filling. However, as the annealed current was increased, the forward current progressively recovered and surpassed its original value. These findings suggest that electropulsing can effectively restore and enhance the functionality of optoelectronic devices by optimizing carrier dynamics and improving performance parameters such as forward current and output power. Further investigations and analyses are necessary to gain deeper insights into the underlying precise micromechanisms driving these observed alterations and to fully understand the potential of electropulsing in the field of optoelectronics.

### Acknowledgments

We acknowledge the funding support from the US National Science Foundation (DMR # 2103928). N.G. acknowledges support from Air Force Office of Scientific Research under Award No. FA9550–19RYCOR050. The views expressed in the article do not necessarily represent the views of the United States Government.

#### ORCID

### References

- 1. A. Liu, P. Wolf, J. A. Lott, and D. Bimberg, *Photon. Res.*, 7, 121 (2019).
- 2. A. V. Babichev et al., IEEE Photonics Technol. Lett., 35, 297 (2023).
- 3. S. Paul et al., *Opt. Express*, **24**, 13142 (2016).
- 4. A. Dehzangi, *Light: Sci. Appl.*, **10**, 17 (2021).
- 5. A. J. Gonsalves et al., Phys. Rev. Lett., 122, 84801 (2019).
- C. Harder, High Power Laser Diodes, ed. R. Diehl (Springer, Berlin, Heidelberg) 1 (2004).
- 7. L. Li and E. A. Carter, J. Am. Chem. Soc., 141, 10451 (2019).
- A. Shluger, Handbook of Materials Modeling, ed. W. Andreoni and S. Yip (Springer International Publishing, Cham) 1013 (2020).
- M. Ohring, The Materials Science of Thin-Films (Academic, New York, NY, USA) (2002).
- L. Freund and S. Suresh, Thin Film Materials: Stress, Defect Formation, and Surface Evolution (Cambridge University Press, UK) (2004).
- 11. A. D. Romig, M. T. Dugger, and P. J. McWhorter, *Acta Mater.*, **51**, 5837 (2003).
- 12. M. Huff, Micromachines, 13, 2084 (2022).
- 13. Y. Zheng, J. Gao, C. Han, and W. Chen, Cell Reports Phys. Sci., 2, 100298 (2021).
- F. Urban, G. Lupina, A. Grillo, N. Martucciello, and A. Di Bartolomeo, *Nano Express*, 1, 10001 (2020).
- 15. D.-B. Zhang, X.-J. Zhao, G. Seifert, K. Tse, and J. Zhu, Natl Sci. Rev., 6, 532 (2019).
- 16. V. Raju, R. PankajNelapati, and K. Sivasankaran, Silicon, 13, 2605 (2021).
- 17. M. Antler, IEEE Circuits Devices Mag., 3, 8 (1987).
- 18. L. Zhang, K. Xu, and F. Wei, J. Mater. Sci., 58, 2087 (2023).
- R. Gunawan, M. Y. L. Jung, E. G. Seebauer, and R. D. Braatz, *J. Process Control*, 14, 423 (2004).
- 20. C. Fu et al., AIP Adv., 7, 35214 (2017).
- P. Lall, M. Pecht, and E. Hakim, Influence of Temperature on Microelectronics and System Reliability (CRC Press, London) (1997).
- P. Lall, A. Abrol, and D. Locker, ASME 2017 International Technical Conference and Exhibition on Packaging and Integration of Electronic and Photonic Microsystems, San Francisco, California, USA, August 29–September 1, 2017 (2017), 10.1115/IPACK2017-74252.
- 23. J. R. Black, IEEE Trans. Electron Devices, 16, 338 (1969).
- 24. I. S. Valeev and Z. G. Kamalov, J. Mater. Eng. Perform., 12, 272 (2003).
- 25. R. A. Fard and M. Kazeminezhad, J. Mater. Res. Technol., 8, 3114 (2019).
- 26. F. Cao, F. Xia, H. Hou, H. Ding, and Z. Li, Mater. Sci. Eng. A, 637, 89 (2015).
- R. Zhang, X. Li, J. Kuang, X. Li, and G. Tang, *Mater. Sci. Technol.*, 33, 1421 (2017).
- 28. H. Conrad, Mater. Sci. Eng. A, 287, 227 (2000).
- A. Haque, J. Sherbondy, D. Warywoba, P. Hsu, and S. Roy, *J. Mater. Process. Technol.*, 299, 117391 (2022).
- 30. M. A. J. Rasel et al., ECS J. Solid State Sci. Technol., 11, 75002 (2022).
- 31. M. A. J. Rasel et al., Appl. Phys. Lett., 122, 204101 (2023).
- 32. V. Kabanov et al., *Semiconductors*, **46**, 1316 (2012).
- 33. X. Zhang et al., Opt. Commun., 537, 129461 (2023).
- 34. K. Häusler, U. Zeimer, B. Sumpf, G. Erbert, and G. Tränkle, *J. Mater. Sci., Mater. Electron.*, 19, 160 (2008).
- 35. S. K. K. Lam, R. E. Mallard, and D. T. Cassidy, J. Appl. Phys., 94, 1803 (2003).
- 36. M. H. Rahman et al., Mater. Res. Express, 10, 116521 (2023).
- 37. A. B. Ikyo et al., Sci Rep., 6, 19595 (2016).
- 38. P. Westbergh et al., Sel. Top. Quantum Electron. IEEE J., 15, 694 (2009).
- 39. J. Zhu, S. Liu, Y. Lin, and G. Wang, J. Mater. Eng. Perform., 29, 841 (2020).
- 40. J. Guo, X. Wang, and W. Dai, Mater. Sci. Technol., 31, 1545 (2015).
- 41. M. Buffolo et al., IEEE J. Sel. Top. Quantum Electron., 26, 1900208 (2020).